Monatshefte für Chemie - Chemical Monthly (2020) 151:1773–1783
https://doi.org/10.1007/s00706-020-02707-1

ORIGINAL PAPER

Disposable biosensors based on platinum nanoparticle-modified screen-printed carbon electrodes for the determination of biogenic amines

Berna Dalkıran[1] · Ceren Kaçar[1] · Erdinç Can[1] · Pınar Esra Erden[2] · Esma Kılıç[1]

Received: 30 June 2020 / Accepted: 22 October 2020 / Published online: 9 November 2020

Abstract

This work presents the development of disposable biosensors used in the determination of biogenic amines. The biosensors were fabricated using diamine oxidase (DAOx) or monoamine oxidase (MAOx) enzyme- and platinum nanoparticle (PtNP)-modified screen-printed carbon electrodes (SPCE). The morphological and electrochemical properties of the biosensors were examined by scanning electron microscopy, energy-dispersive X-ray spectroscopy, electrochemical impedance spectroscopy, and cyclic voltammetry measurements. Amperometric measurements indicated that the DAOx/PtNP/SPCE biosensor responded to histamine, putrescine, cadaverine, spermine, spermidine, *β*-phenylethylamine, tryptamine, and tyramine; however, its MAOx-based counterpart showed no response towards putrescine and cadaverine. A performance comparison of two biosensors indicated that the one based on DAOx had a linear concentration range from 5.3×10^{-7} to 7.2×10^{-5} M and the other based on MAOx from 3.9×10^{-7} to 7.6×10^{-5} M for tyramine. The sensitivities of the DAOx- and MAOx-based biosensors towards tyramine were 24.8 µA mM^{-1} and 46.1 µA mM^{-1}, respectively. The proposed biosensors were tested for analysis of blue cheese sample spiked with known concentration of tyramine for the verification of biosensor applicability for real samples.

Graphic abstract

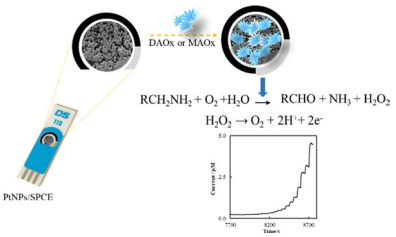

Keywords Biogenic amines · Amperometric biosensor · Screen-printed electrode · Platinum nanoparticles · Diamine oxidase · Monoamine oxidase

Introduction

Biogenic amines (BAs) are low molecular weight organic bases. These amines are mainly formed as a consequence of microbial decarboxylation of amino acids [1, 2]. The main BAs present in food products are histamine, putrescine, cadaverine, spermine, spermidine, *β*-phenylethylamine, tryptamine, and tyramine [3]. Biogenic amine formation in food products may occur due to inappropriate processing and

✉ Esma Kılıç
ekilic@science.ankara.edu.tr

[1] Department of Chemistry, Faculty of Science, Ankara University, 06100 Ankara, Turkey

[2] Department of Chemistry, Polatlı Faculty of Science and Arts, Ankara Hacı Bayram Veli University, 06900 Ankara, Turkey

storage conditions and subsequent microbial contamination. Therefore, the level of BAs in food can be used as a chemical indicator of spoilage [4]. Moreover, the ingestion of food containing high amounts of these amines can cause health problems [5]. The level of BAs in food products needs to be strictly controlled due to their toxicological risk and importance in food quality. For these reasons, the development of rapid, accurate, and practical methods for BA determination is becoming increasingly demanded.

Various analytical methods such as high-performance liquid chromatography [6], thin layer chromatography [7], gas chromatography [8], capillary zone electrophoresis [9] and electrochemical sensor and biosensors [10–14] have been reported to monitor the level of BAs. Amperometric biosensors offer several advantages over traditional chromatographic techniques for BA determination in terms of low cost, rapid response, high sensitivity and construction simplicity [15, 16]. Due to these reasons, nowadays, there is a great interest in the development of practical and reliable biosensors for the analysis of food products to guarantee their composition, safety, quality and traceability in accordance with regulatory legislation and consumer demands [17, 18].

The biosensors reported for the determination of BAs are generally based on the use of amine oxidase enzymes. These enzymes catalyze the conversion of the biogenic amines to the corresponding aldehyde, NH_3, and H_2O_2 [19]. In these biosensors, the consumption of O_2 [20] or the generation of H_2O_2 [21] can be monitored to quantify BAs.

Metal nanoparticles (MNP), especially gold and platinum nanoparticles (PtNP), have been widely used in the fabrication of electrochemical biosensors to improve their analytical performance characteristics [22, 23]. This is because MNP exhibit unique properties such as large effective surface area, strong catalytic properties that facilitate electron transfer between the electrode surface and biomolecule, good adsorption ability for biomolecule immobilization, and high surface activity [23]. Previous studies have indicated that PtNP possess excellent catalytic capabilities towards the oxidation and reduction of H_2O_2 [24]. Moreover, PtNP can provide biocompatible platforms for enzymes which is important for keeping their biologic activities [25].

Disposable screen-printed electrodes (SPEs) are planar sensor systems fabricated by the printing of conductive ink onto ceramic or plastic support [26]. They have important advantages such as mass production capabilities, low cost, portability, and practical use [27]. The modification of SPEs with MNP is a practical approach for the development of more sensitive amperometric biosensors [26].

Herein we report the construction and application two biogenic amine biosensors based on DAOx or MAOx enzyme- and PtNP-modified SPCEs for the rapid, practical, sensitive, and selective analysis of BAs. A comparison of the analytical performances of two biogenic amine biosensors is also presented and discussed. PtNP were grown on SPCEs using a one-step electrodeposition process and these electrodes were then modified with DAOx or MAOx for the development of the biosensors. The experimental conditions which can effect the biosensors performance were optimized and the analytical characteristics of both biosensors were described. The practical use of both biosensors in real-sample analysis was also performed.

Results and discussion

Optimization of electrode surface composition

The electrodeposition of PtNP on SPCE was performed in an electroplating bath consisted of 2 mM H_2PtCl_6 and 0.1 M HCl [28], making a total volume of 5 cm^3. The bare SPCE was immersed in the plating bath, and a constant potential was applied under stirring condition. To optimize the electrodeposition step, constant potentials of − 0.20 V, − 0.30 V, and − 0.40 V and time intervals of 450 and 300 s were investigated. DAOx was immobilized onto all electrodes fabricated with different platinum electrodeposition procedures and tyramine responses of these biosensors were investigated. The highest tyramine response was obtained with the biosensor fabricated with the modified electrode at which platinum was electrodeposited at a constant potential of − 0.40 V for 450 s. Therefore, these conditions were selected as the optimal for the PtNP electrodeposition.

Surface morphology

Scanning electron microscopy (SEM) was used to characterize the morphologies of (a) bare SPCE, (b) PtNP/SPCE, (c) DAOx/PtNP/SPCE, and (d) MAOx/PtNP/SPCE electrodes during stepwise modification. As shown in Fig. 1b, after the electrodeposition of PtNP, the nanoparticles covered the electrode surface and PtNP/SPCE had larger surface compared with the bare SPCE (Fig. 1a). Moreover, the spherical structure of the electrodeposited PtNP can be observed at electrode surface. The corresponding image slightly changed and a cloudy appearance was obtained when DAOx was immobilized on PtNP/SPCE (Fig. 1c). After the immobilization of MAOx onto PtNP/SPCE, the SEM image changed significantly (Fig. 1d). These changes observed in SEM images of enzyme modified electrodes can be attributed to the immobilization of the enzymes onto the electrode surface. Similar results were reported in the literature for DAOx- and MAOx-modified electrodes [14, 16].

Energy-dispersive X-ray spectroscopy (EDX) analysis was utilized to investigate the surface composition of PtNP/SPCE. Figure 1e depicts the EDX spectrum of PtNP/SPCE.

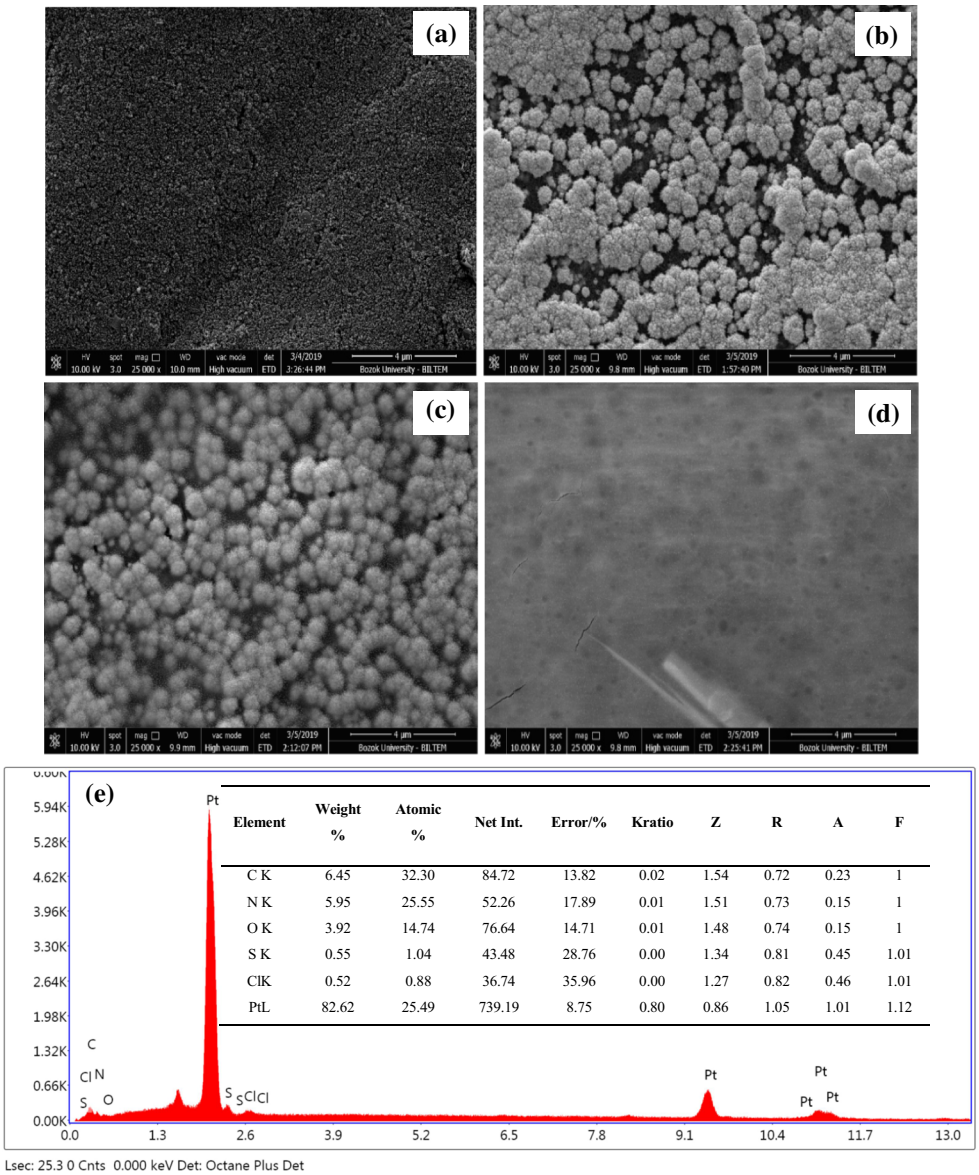

Element	Weight %	Atomic %	Net Int.	Error/%	Kratio	Z	R	A	F
C K	6.45	32.30	84.72	13.82	0.02	1.54	0.72	0.23	1
N K	5.95	25.55	52.26	17.89	0.01	1.51	0.73	0.15	1
O K	3.92	14.74	76.64	14.71	0.01	1.48	0.74	0.15	1
S K	0.55	1.04	43.48	28.76	0.00	1.34	0.81	0.45	1.01
ClK	0.52	0.88	36.74	35.96	0.00	1.27	0.82	0.46	1.01
PtL	82.62	25.49	739.19	8.75	0.80	0.86	1.05	1.01	1.12

Fig. 1 SEM images of **a** bare SPCE, **b** PtNP/SPCE, **c** DAOx/PtNP/SPCE, and **d** MAOx/PtNP/SPCE. **e** EDX spectrum and elementel analysis (inset table) of PtNP/SPCE

The peak corresponding to the Pt element indicated that the PtNP were successfully electrodeposited on the surface of bare SPCE, which supports the SEM results.

Electrochemical characteristics of the modified electrodes

Cyclic voltammetry (CV) and electrochemical impedance spectroscopy (EIS) were used to characterize the modification of the electrode in 5 mM $Fe(CN)_6^{3-/4-}$ and 0.1 M KCl solution. Figure 2 compares the CV response at bare SPCE (a) and PtNP/SPCE (b) obtained at a scan rate of 50 mV s^{-1} in the above solution, respectively. At the bare SPCE (curve a), oxidation and reduction peaks corresponding to the redox behaviour of ferricyanide–ferrocyanide couple was observed with a peak to peak separation (ΔEp) of 288 mV. After modified with PtNP, the anodic and cathodic peak currents were increased (curve b), indicating PtNP can improve the surface area of the electrode [29]. The electroactive surface area of the electrodes was estimated with CV according to the Randles–Sevcik equation [30]:

$$i_p = 2.69 \times 10^5 A D^{1/2} n^{3/2} v^{1/2} C.$$

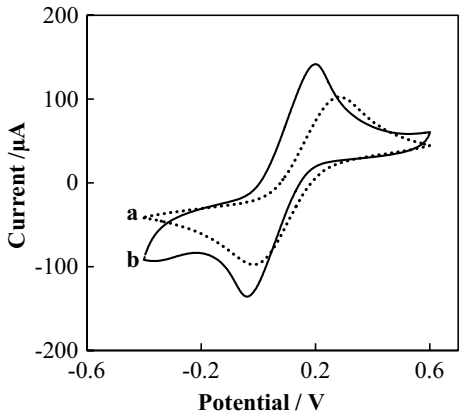

Fig. 2 Cyclic voltammograms of **a** SPCE and **b** PtNP/SPCE (in 0.1 M KCl and 5.0 mM $Fe(CN)_6^{3-/4}$ at 50 mV s^{-1} scan rate)

In this equation, n is the number of electrons transferred ($n=1$), A refers to the electroactive surface area of the electrode (cm^2). D is the diffusion coefficient of the molecule in solution (6.7×10^{-6} cm^2 s^{-1}), ν refers to the scan rate (0.05 V s^{-1}) and C is the concentration of the prob molecule in the bulk solution (5 mM). By applying the Randles–Sevcik equation, the calculated electroactive surface areas were 0.114 cm^2 and 0.164 cm^2 for SPCE and PtNP/SPCE, respectively. In comparison with the bare SPCE, the electroactive surface area of the PtNP/SPCE was increased by about 1.4 times. Furthermore, the peak to peak separation ($\Delta Ep=239$ mV) decreased suggesting that the modification of the electrode surface with PtNP increased the electron transfer between the electrode surface and solution due to the increase in surface to volume ratio as a result of large surface area provided by the PtNP.

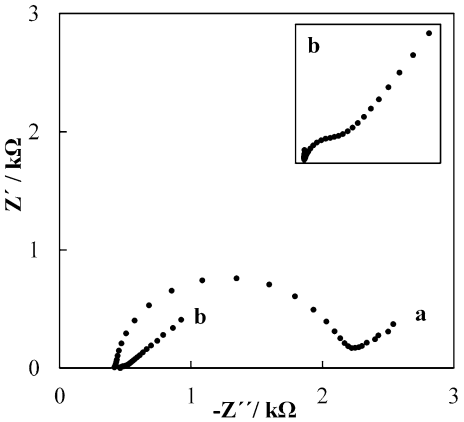

Fig. 3 EIS of **a** SPCE and **b** PtNP/SPCE (in 0.1 M KCl and 5.0 mM $Fe(CN)_6^{3-/4-}$)

Figure 3 displays the EIS of the electrodes obtained in 5 mM $Fe(CN)_6^{3-/4-}$ and 0.1 M KCl solution. It can be seen from the figure that the electron transfer resistance (semicircle diameter, R_{ct}) value of bare SPCE (1660 Ω) (curve a) remarkably decreased when the electrode was modified with PtNP (35.2 Ω) (curve b). This result indicates that the PtNP form high electron conduction pathways between the electrode and electrolyte and obviously improve the diffusion of ferricyanide toward the electrode surface [31].

Optimization of experimental parameters

Working potential

Amine oxidase enzymes catalyze the conversion of the biogenic amines to the corresponding aldehyde, NH_3, and H_2O_2. H_2O_2 enzymatically generated from the BAs in the presence of DAOx or MAOx (Eq. (1)) is oxidized to O_2 (Eq. (2)), and the current response obtained is directly proportional to the concentration of the corresponding biogenic amine [32]. The electrochemical reactions involved in response mechanism of the DAOx/PtNP/SPCE and MAOx/PtNP/SPCE biosensors are given below:

$$RCH_2NH_2 + O_2 + H_2O \rightarrow RCHO + H_2O_2 + NH_3 \text{ (in the presence of DAOx or MAOx)}, \quad (1)$$

$$H_2O_2 \rightarrow O_2 + 2H^+ + 2e^- (+0.50\ V). \quad (2)$$

The working potential has a great effect on biosensor performance since it contributes to its sensitivity and selectivity. Figure 4 shows the cyclic voltammograms of (a) SPCE, (b) PtNP/SPCE, and (c) DAOx/PtNP/SPCE

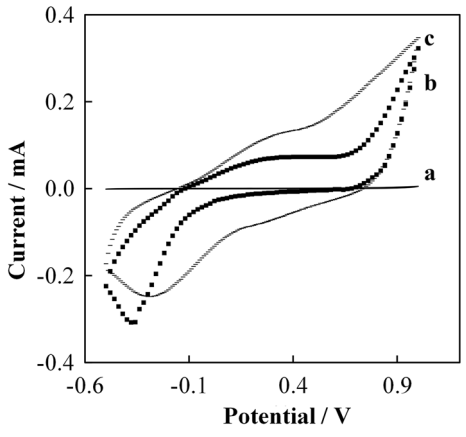

Fig. 4 Cyclic voltammograms of **a** SPCE, **b** PtNP/SPCE, and **c** DAOx/PtNP/SPCE in 0.1 mM H_2O_2 (0.05 M, pH 7.0, BR buffer solution containing 0.1 M KCl)

taken in 0.05 M BR buffer solution containing 0.1 M KCl (pH 7.0) and 0.1 mM H_2O_2 at a scan rate of 50 mV s^{-1}. As can be seen the peak currents recorded at PtNP/SPCE and DAOx/PtNP/SPCEs are higher than the currents recorded at SPCE and the oxidation process of H_2O_2 starts at about + 0.40 V.

Due to the CV results, the amperometric response of DAOx/PtNP/SPCE to tyramine was investigated at a constant tyramine concentration of 0.02 mM between + 0.20 and + 0.60 V to determine the optimum working potential (Fig. 5). The response current increased as the potential becomes more positive from + 0.20 to + 0.60 V, and the highest sensitivity was obtained at + 0.60 V. However, a working potential of + 0.50 V was selected as the working potential to decrease the effect of possible interferences.

pH

DAOx and MAOx enzymes catalyze the oxidative deamination of various BAs. Therefore, the influence of buffer pH on the amperometric responses of DAOx/PtNP/SPCE and MAOx/PtNP/SPCE biosensors was investigated in 0.05 M BR buffer solution at constant biogenic amine concentration for various BAs (histamine, cadaverine, putrescine, *β*-phenylethylamine, tryptamine, tyramine, spermine, and spermidine) widely present in food products. For the DAOx/PtNP/SPCE biosensor, optimum pH was found to be 8.0 for histamine and putrescine; 7.5 for cadaverine; 8.5 for tryptamine; 8.0 for tyramine; 8.5 for spermine, and *β*-phenylethylamine and 10.5 for spermidine (Fig. 6).

In case of MAOx/PtNP/SPCE biosensor, pH 7.5 for tryptamine, 9.5 for tyramine, spermine, and *β*-phenylethylamine, and 10.0 for histamine and spermidine were obtained as the optimum values for the buffer pH. These optimum pH values were used in the determination of analytical characteristics of both biosensors and chronoamperometric responses were measured at optimum pH of each amine.

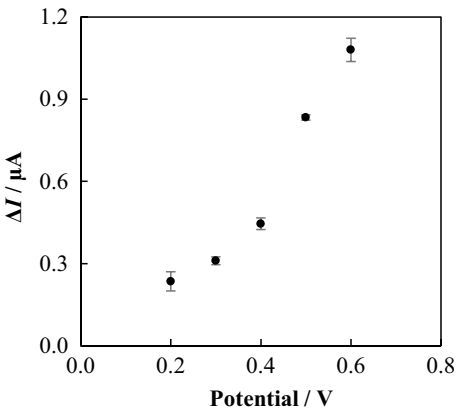

Fig. 5 Effect of working potential on the response of DAOx/PtNP/SPCE biosensor (pH 8.0, BR buffer solution in the presence of 0.02 mM tyramine)

Performance parameters and substrate specificity

Chronoamperometry was used to determine the responses of DAOx/PtNP/SPCE and MAOx/PtNP/SPCE biosensors to histamine, cadaverine, putrescine, *β*-phenylethylamine, tryptamine, tyramine, spermine, and spermidine and *i*–*t* graphs were recorded for each biogenic amine at its optimum pH. Figure 7 depicts the amperometric responses of DAOx/PtNP/SPCE and MAOx/PtNP/SPCE biosensors to consecutive additions of tyramine at + 0.50 V and the corresponding calibration curves of the calculated current differences (ΔI) vs. the concentration of tyramine determined by both biosensors. DAOx/PtNP/SPCE biosensor displayed a linear relationship between the current and tyramine concentration in the range of 5.3×10^{-7}–7.2×10^{-5} M with a sensitivity of 24.8 μA mM^{-1}. The limit of detection (LOD) was calculated according to the $3s_b/m$ criteria, where m represents the slope of the calibration graph and s_b represents the standard deviation of the amperometric responses from different solutions of tyramine at the concentration level corresponding to the lowest concentration of the calibration curve [33, 34]. The LOD of the DAOx-based biosensor was found to be 2.5×10^{-7} M for tyramine. For the MAOx/PtNP/SPCE biosensor, the linear dynamic range of the tyramine determination was from 3.9×10^{-7}–7.6×10^{-5} M. The detection limit and sensitivity of this biosensor were found to be 2.1×10^{-7} M and 46.1 μA mM^{-1}, respectively. Both biosensors exhibited a rapid electrochemical response, reaching 95% of the steady-state current within 5 s after each tyramine addition.

Table 1 presents the linear dynamic ranges and sensitivities obtained from corresponding calibration graphs for all BAs investigated. As can be seen from the table, both biosensors exhibited a wide linear working range and good sensitivity for tyramine determination. DAOx/PtNP/SPCE biosensor showed the highest sensitivity to spermine (39.8 μA mM^{-1}) with a linear dynamic range of 3.8×10^{-7}–9.9×10^{-6} M and LOD of 1.1×10^{-7} M. This biosensor also exhibited high sensitivity to spermidine (37.7 μA mM^{-1}) with a wider linear dynamic range of 2.9×10^{-7}–4.6×10^{-5} M. Although a very narrow linear dynamic range (2.7×10^{-6}–9.8×10^{-5} M) was obtained for tryptamine, the sensitivity of 24.2 μA mM^{-1} was quite satisfactory. This biosensor responded to histamine (5.2 μA mM^{-1}), putrescine (4.5 μA mM^{-1}), and cadaverine (5.4 μA mM^{-1}) with a lower sensitivity. However, wide linear dynamic ranges were obtained for histamine (3.8×10^{-7}–1.1×10^{-5} M), putrescine (4.9×10^{-7}–2.3×10^{-5} M), and cadaverine

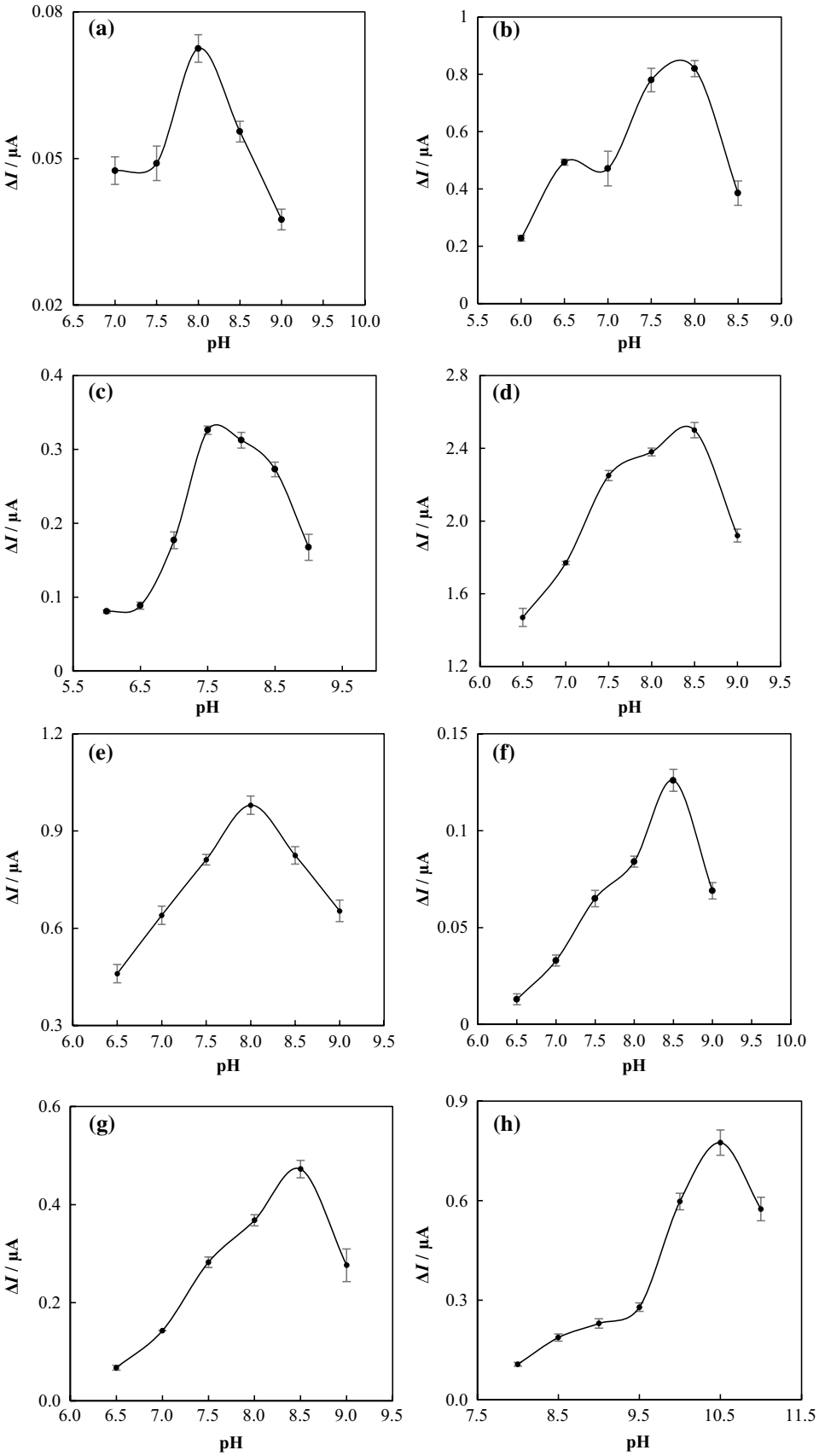

Fig. 6 Effect of buffer pH on the **a** histamine, **b** putrescine, **c** cadaverine, **d** tryptamine, **e** tyramine, **f** β-phenylethylamine, **g** spermine, and **h** spermidine response of DAOx/PtNP/SPCE biosensor (in 0.05 M BR buffer at + 0.50 V. The error bars are calculated from measurements performed with three different biosensors)

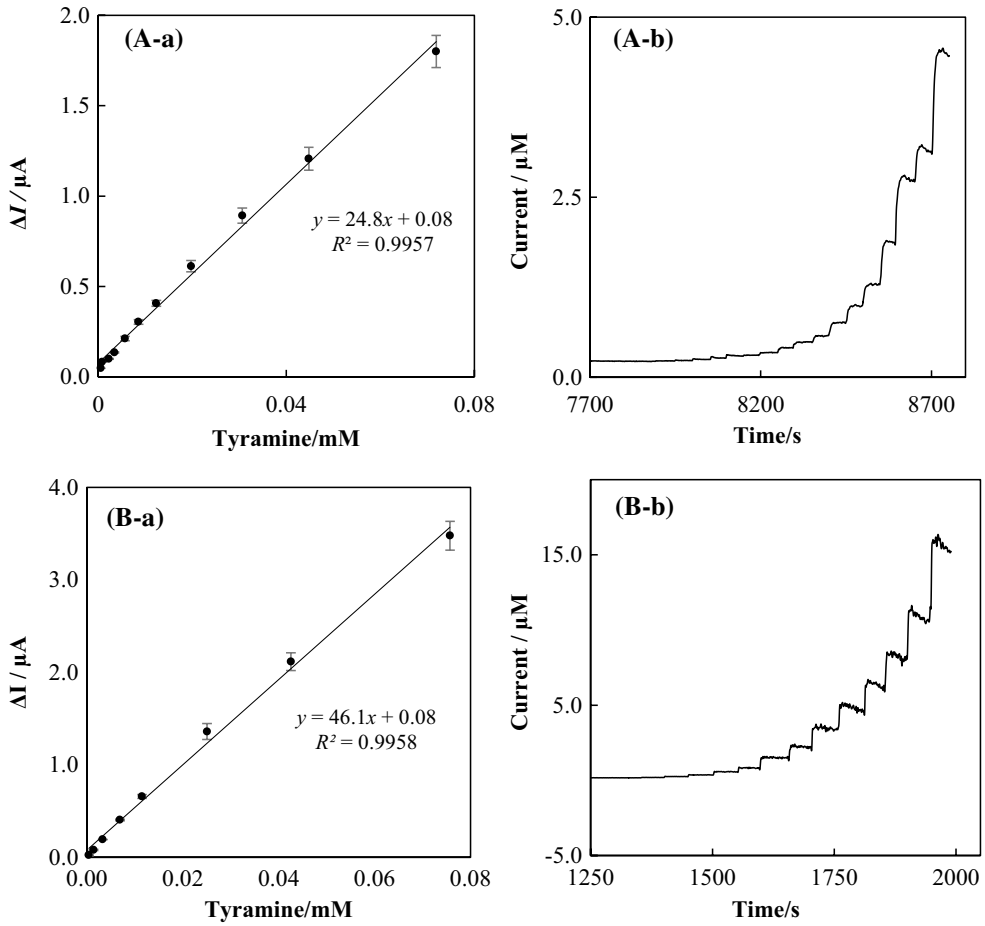

Fig. 7 **a** Calibration curves and **b** chronoamperometric *i–t* graphs of **A** DAOx/PtNP/SPCE (pH 8.0) and **B** MAOx/PtNP/SPCE (pH 9.5) for tyramine in 0.05 M BR buffer at + 0.50 V. The error bars are calculated from measurements performed with three different biosensors

Table 1 Analytical performance characteristics of DAOx/PtNP/SPCE and MAOx/PtNP/SPCE biosensors for various biogenic amines obtained at + 0.50 V in 0.05 M BR buffer solution

Substrate	DAOx/PtNP/SPCE				MAOx/PtNP/SPCE			
	pH	Linear dynamic range/M/R^2	LOD/M	Sensitivity/ μA mM^{-1}	pH	Linear dynamic range/M/R^2	LOD/M	Sensitivity/ μA mM^{-1}
Histamine	8.0	3.8×10^{-7}–1.1×10^{-5}/ 0.9877	3.8×10^{-7}	5.2	10.0	3.3×10^{-6}–4.9×10^{-5}/ 0.986	2.7×10^{-7}	1.9
Putrescine	8.0	4.9×10^{-7}–2.3×10^{-5}/ 0.9846	4.7×10^{-7}	4.5	–	–	–	–
Cadaverine	7.5	9.0×10^{-7}–1.1×10^{-5}/0.9946	8.4×10^{-7}	5.4	–	–	–	–
Tryptamine	8.5	2.7×10^{-6}–9.8×10^{-5}/ 0.9963	2.4×10^{-7}	24.2	7.5	7.9×10^{-8}–8.0×10^{-3}/ 0.9864	5.2×10^{-8}	38.6
Tyramine	8.0	5.3×10^{-7}–7.2×10^{-5}/ 0.9957	2.5×10^{-7}	24.8	9.5	3.9×10^{-7}–7.6×10^{-5}/ 0.9958	2.1×10^{-7}	46.1
β-Phenylethylamine	8.5	9.5×10^{-6}–10.8×10^{-4}/ 0.9924	2.5×10^{-6}	0.9	9.5	2.4×10^{-5}–5.9×10^{-4}/ 0.986	1.8×10^{-5}	0.6
Spermine	8.5	3.8×10^{-7}–9.9×10^{-6}/ 0.993	1.1×10^{-7}	39.8	9.5	4.9×10^{-7}–1.6×10^{-4}/ 0.9885	2.3×10^{-7}	18.1
Spermidine	10.5	2.9×10^{-7}–4.6×10^{-5}/ 0.9838	2.8×10^{-7}	37.7	10.0	7.9×10^{-7}–1.0×10^{-4}/ 0.9887	3.9×10^{-7}	32.3

(9.0×10^{-7}–1.1×10^{-5}). DAOx/PtNP/SPCE biosensor showed the lowest sensitivity to β-phenylethylamine (0.9 μA mM^{-1}) with a linear dynamic range of 9.5×10^{-6}–1.8×10^{-4} M. It can be concluded that DAOx/PtNP/SPCE biosensor can be used in the determination of all BAs investigated.

In case of MAOx/PtNP/SPCE biosensor, no response was obtained for putrescine and cadaverine. Contrary to DAOx/PtNP/SPCE biosensor, a very wide linear dynamic range of 7.9×10^{-8}–8.0×10^{-3} M was obtained with MAOx-based biosensor for tryptamine with a high sensitivity of 38.6 μA mM^{-1}. On the other hand, this biosensor responded to spermine (18.1 μA mM^{-1}; 4.9×10^{-7}–1.6×10^{-4} M) and spermidine (32.3 μA mM^{-1}; 7.9×10^{-7}–1.0×10^{-4} M) with good sensitivity and wide linear dynamic range. However, the lower sensitivities and narrow linear ranges were obtained for histamine (1.9 μA mM^{-1}; 3.3×10^{-6}–4.9×10^{-5} M) and β-phenylethylamine (0.6 μA mM^{-1}; 2.4×10^{-5}–5.9×10^{-4} M). These results indicated that MAOx based can be used in the determination of histamine, β-phenylethylamine, tryptamine, tyramine, spermine, and spermidine.

The repeatability and reproducibility of the DAOx/PtNP/SPCE and MAOx/PtNP/SPCE biosensors were explored using tyramine as a substrate. Five successive calibration curves were plotted under the optimum experimental conditions using the same biosensor to evaluate the repeatability. The change observed in sensitivities between the 1st and the 5th calibration in terms of relative standard deviation (RSD) was 8% and 6% for with DAOx/PtNP/SPCE and MAOx/PtNP/SPCE biosensors, respectively. This result indicated the satisfactory repeatability of the biosensors. In case of reproducibility, calibration curves were obtained, using five different similarly fabricated electrodes. The RSD values obtained with DAOx/PtNP/SPCE and MAOx/PtNP/SPCE biosensors were 6.5% and 4.9%, respectively. It can be concluded that the biosensors exhibited good reproducibility. The operational stability of the presented biosensors was also investigated by the measurements of the biosensor response to 0.02 mM tyramine. The presented DAOx/PtNP/SPCE (RSD < 10%) and MAOx/PtNP/SPCE (RSD < 7%) biosensors showed good operational stability after 30 successive measurements.

Table 2 shows the analytical characteristics of various previously reported biogenic amine biosensors. A comparison of the data presented in Tables 1 and 2 indicates that DAOx/PtNP/SPCE and MAOx/PtNP/SPCE biosensors offered a higher sensitivity and lower detection limit for the BAs investigated than most of the previous biogenic amine biosensors.

Interference effect

The interference effect of various amino acids on the tyramine response of the biosensors (histidine, ornithine, tyrosine, lysine, tryptophan, arginine, and β-phenylethylamine) was investigated. The amino acids studied were those involved in the biosynthesis of BAs [19]. The interference effect was determined by comparison of the response obtained for 0.1 mM standard tyramine solution vs. the response obtained for the same concentration of standard amino acid solutions and presented in Table 3 in terms of interference percentage.

As seen from the Table, β-phenylethylamine showed a slight effect (< 3%) on the response of DAOx/PtNP/SPCE and MAOx/PtNP/SPCE biosensors. The interference effect of tyrosine, arginine, histidine, and ornithine was < 10% at both biosensors. In case of lysine 12.0% interference was observed for DAOx/PtNP/SPCE. However, the effect of lysine was smaller at MAOx/PtNP/SPCE (11.3%). On the other hand, tryptophan caused 23.4% and 28.3% interference on the tyramine response currents of DAOx/PtNP/SPCE and MAOx/PtNP/SPCE biosensors, respectively. This high interference effect of tryptophan can be attributed to its electrochemical oxidation at the operating potential [38]. It can be concluded that the presence of tryptophan in real samples can affect the tyramine response of the biosensor.

Real-sample analysis

The performance of the DAOx/PtNP/SPCE vs. MAOx/PtNP/SPCE biosensors was evaluated using cheese sample that spiked with known concentrations of tyramine. Tyramine was selected as the reference amine for the recovery tests due to the high sensitivities and wide linear dynamic ranges obtained with both biosensors for tyramine. Moreover, tyramine is one of the most common BAs present in cheese. For this purpose, 50 mm^3 of the cheese extract was added to the electrochemical cell containing 5 cm^3 of BR buffer solution and standard addition was performed to determine the tyramine level in cheese sample. However, both biosensors detected no tyramine in cheese sample. Therefore, the recovery tests were performed by spiking certain amounts of standard tyramine solution to the cheese extract to investigate the applicability of the presented biosensors. The tyramine levels in spiked sample were determined by standard addition method in triplicate. The recoveries of tyramine from spiked cheese sample determined by both biosensors are presented in Table 4. The recoveries obtained for tyramine were about 100%, indicating that the reliability of the biosensor method is good, and the developed biosensors can be used for tyramine determination in cheese samples.

Table 2 Some analytical characteristics of previously reported biogenic amine biosensors

Modification	Applied potential/V	BAs	Linear range/μM	LOD/μM	Sensitivity/ μA mM^{-1}	Real sample	References
DAOx/1,4-DAB/Pt	+0.65	Histamine	1–1000	0.5	0.0182	BAs in cheese	[35]
		Putrescine	1–1000	0.5	0.0146		
		Cadaverine	5–1000	0.1	0.0110		
		Tryptamine	5–200	2	0.0059		
		Tyramine	1–100	0.5	0.0170		
		β-Phenylethylamine	1–200	0.5	0.0150		
PSAO/MnO_2/SPCE	+0.40	Histamine	10–300	3	0.00046	BAs in chicken meat	[36]
		Putrescine	1–50	0.3	0.00595		
		Cadaverine	1–50	0.3	0.00828		
		Tyramine	10–300	3	0.00043		
DAOx-MB/CoPTH/carbon	+0.40	Histamine	10–1000	5.13	0.13	–	[37]
		Putrescine		1.03	2.11		
		Cadaverine		0.60	3.03		
DAOx-MB/PB/carbon	− 0.10	Histamine	10–1000	4.80	0.57	Histamine in fish	
		Putrescine		0.90	3.22		
		Cadaverine		0.67	3.12		
DAOx-MB/Os-wired HRP/ carbon	+0.50	Histamine	10–1000	4.50	0.31	–	
		Putrescine		0.90	3.31		
		Cadaverine		0.47	2.61		
DAOx/ITONP/PB/SPCE	− 0.15	Histamine	6–690	1.9	1.84	Histamine in cheese	[14]
		Putrescine	7.9–3000	7.8	0.44		
		Cadaverine	6–3000	2.7	0.65		
MAOx/ITONP/PB/SPCE	− 0.15	Histamine	$2–3.2\times10^4$	2	0.06	Cadaverine in cheese	
		Putrescine	4–120	3.8	0.22		
			2.9–3900	2.9	0.03		
		Cadaverine	3–1000	0.89	0.57		
DAOx/PVF/GRO/SPCE	+0.50	Histamine	50–740	27	0.10	Tyramine in cheese	[16]
		Putrescine	99–1100	67	0.10		
		Cadaverine	99–1600	43	0.05		
		Tryptamine	6–340	1.4	3.66		
		Tyramine	0.99–120	0.41	7.99		
		β-Phenylethylamine	39–510	9	0.21		
		Spermine	200–1100	92	0.16		
		Spermidine	65–660	15	0.20		
MAOx/PVF/GRO/SPCE	+0.50	Tryptamine	2.4–120	1.8	7.51	Tyramine in cheese	
		Tyramine	0.99–110	0.61	11.98		
		β-Phenylethylamine	50–1200	38	0.05		
		Spermine	99–1200	22	0.12		
		Spermidine	99–1500	54	0.13		

1,4-DAB 1,4-diamminebenzene, *PSAO* pea seedling amine oxidase, *SPCE* screen-printed carbon electrode, *MB* magnetic beads, *CoPHT* Co(II)-phthalocyanine, *ITONP* indium-tin-oxide nanoparticles, *PB* Prussian blue, *PVF* poly(vinylferrocene), *GRO* graphene oxide

Conclusion

Two amperometric biosensors based on DAOx- or MAOx-immobilized PtNP-modified SPCEs were developed for the determination of BAs and their analytical performance characteristics were compared. DAOx/PtNP/SPCE biosensor responded to all BAs investigated; however, its MAOx-based counterpart did not respond to putrescine and cadaverine. MAOx/PtNP/SPCE biosensor showed the highest sensitivity to tyramine which was 1.9 times higher than the sensitivity obtained with DAOx-based biosensor. Both biosensors showed low sensitivity to *β*-phenylethylamine and the linear dynamic range obtained with DAOx/PtNP/SPCE for tryptamine was narrow. DAOx/PtNP/SPCE and MAOx/PtNP/SPCE biosensors exhibited higher sensitivity and lower detection limit for the BAs than most of the

Table 3 Effect of various amino acids on the tyramine response of DAOx/PtNP/SPCE and MAOx/PtNP/SPCE biosensors (in 0.05 M BR buffer, $E_{app} = +0.50$ V)

Amino acid	DAOx/PtNP/SPCE Interference/%	MAOx/PtNP/SPCE Interference/%
Tyrosine	8.7	6.5
Tryptophan	23.4	28.3
Arginine	− 8.4	− 5.9
Lysine	− 12.0	− 11.3
Histidine	− 9.4	− 8.7
Ornithine	− 5.7	− 6.4
Phenylalanine	− 2.4	− 2.1

earlier biogenic amine biosensors. Moreover, these biosensors possess the advantage of easy and rapid construction and which is critical in routine analysis. The presented biosensors successfully applied for tyramine determination in spiked cheese sample and good recoveries were obtained.

Experimental

Human recombinant MAOx A (≥ 10 unit/mg protein, ≥ 3 mg protein/cm^3, EC 1.4.3.4.), DAOx from porcine kidney (≥ 0.05 unit/mg solid, EC 1.4.3.22), histamine dihydrochloride, potassium chloride, chloroplatinic acid ($H_2PtCl_6 \cdot 6H_2O$), cadaverine dihydrochloride, β-phenylethylamine hydrochloride, spermine, spermidine, tryptamine, putrescine dihydrochloride, tyramine, boric acid, acetic acid, phosphoric acid, potassium hexacyanoferrate(III), potassium hexacyanoferrate(II) trihydrate, Nafion® perfluorinated resin solution, L-histidine, L-tyrosine, L-tryptophan, L-arginine, L-lysine, and L-phenylalanine were supplied from Sigma-Aldrich (Sigma-Aldrich, USA). L-Ornithine hydrochloride was purchased Acros Organics. Deionized water obtained from ELGA Purelab Option-S System was used throughout the experiments. SPCEs with working electrodes of 4 mm in diameter (model C110) were bought from Dropsens (Llanera, Spain).

The electrodeposition of PtNP and electrochemical measurements were performed using an Ivium CompactStat electrochemical analyzer (Ivium Technologies, Netherlands) at room temperature. The amperometric measurements were carried out at + 0.50 V in 0.05 M Britton–Robinson (BR) buffer solution. After the working electrode reached the steady state (background current), aliquots of tyramine stock solution were successively added to the stirred BR buffer and the steady-state current values recorded. In amperometric measurements, the variation (Δi) between the steady-state current and background current was marked as the response current. Cyclic voltammetry and electrochemical impedance spectroscopy measurements were obtained in the presence of 5.0 mM $K_3[Fe(CN)_6]/K_4[Fe(CN)_6]$ (1:1) and 0.1 M KCl solution. A frequency range of 100 kHz−0.1 Hz was utilized with a potential amplitude of 5 mV for the EIS measurements. Scanning electron microscopy images and energy-dispersive X-ray spectroscopy spectra were obtained by using FEI, Quanta 450 FEG model scanning electron microscope, and Bruker detector, respectively.

Fabrication of the biosensors

The SPCE was immersed in 1.0 M H_2SO_4 solution and activated by electrochemical cyclic scanning method with 5 scans at a scanning speed of 100 mV s^{-1} and potential range from − 0.40 to + 0.60 V. Electrodeposition of PtNP on SPCE was carried out in an electroplating bath containing 2 mM H_2PtCl_6 and 0.1 M HCl. The activated SPCE was immersed in the plating bath, and a constant potential of − 0.40 V was applied for 450 s. For the fabrication of the biogenic amine biosensors, 5 mg of DAOx was dissolved in 1 cm^3 of 0.05 M BR buffer solution (pH 7.2) (1.0 U cm^{-3}) and 5 mm^3 of the enzyme solution was pipetted on the surface of the PtNP/SPCE. After drying for 2 h at 4 ℃ in refrigerator, a 0.25% Nafion solution was dropped on the electrode surface as a protective membrane. In case of MAOx-based biosensor, 5 mm^3 enzyme (30 U cm^{-3}) was immobilized onto the PtNP/SPCE surface and the electrode surface was further modified with Nafion solution for the fabrication of the biosensor.

Table 4 Recoveries of tyramine from cheese obtained with DAOx/PtNP/SPCE and MAOx/PtNP/SPCE biosensors

DAOx/PtNP/SPCE			MAOx/PtNP/SPCE		
Tyramine added/ mg dm^{-3}	Tyramine found/ mg dm^{-3}	Recovery/%	Tyramine added/ mg dm^{-3}	Tyramine found/ mg dm^{-3}	Recovery/%
4.59	4.76 ± 0.04	103.3 ± 0.6	3.96	4.24 ± 0.3	103.5 ± 4.9
6.96	7.05 ± 0.05	101.3 ± 0.6	6.22	6.31 ± 0.3	101.6 ± 5.7
9.36	9.21 ± 0.1	98.7 ± 0.7	8.65	8.45 ± 0.2	97.8 ± 1.5
Average recovery 100.4 ± 2.4			Average recovery 101.0 ± 4.6		

Sample preparation

2 g of blue cheese sample obtained from a local market was weighed and homogenized. 10 cm^3 of 0.40 M $HClO_4$ was added to the homogenate and blended for 10 min. The blend was centrifuged for 10 min at 4100 rpm. The supernatant was diluted to 1:25 with BR buffer solution and the cheese was stored at − 18 ℃ in refrigerator.

Acknowledgements We gratefully acknowledge the financial support (TUBITAK Project no.: 116Z159) of The Scientific and Technological Research Council of Turkey.

References

1. Önal A (2007) Food Chem 103:1475
2. Nalazek-Rudnicka K, Wasik A (2017) Monatsh Chem 148:1685
3. Erim FB (2013) TrAC Trends Anal Chem 52:239
4. Jairath G, Singh PK, Dabur RS, Rani M, Chaudhari M (2015) J Food Sci Technol 52:6835
5. Alvarez MA, Moreno-Arribas MV (2014) Trends Food Scı Tech 39:146
6. Peng JF, Fang KT, Xie DH, Ding B, Yin JY, Cui XM, Zhang Y, Liu JF (2008) J Chromatogr A 1209:70
7. Tao Z, Sato M, Han Y, Tan Z, Yamaguchi T, Nakano T (2011) Food Control 22:1154
8. Önal A, Tekkeli SEK, Önal C (2013) Food Chem 138:509
9. Kvasnička F, Voldřich M (2006) J Chromatogr A 1103:145
10. Henao-Escobar W, Del Torno-de RL, Domínguez-Renedo O, Alonso-Lomillo MA, Arcos-Martínez MJ (2016) Food Chem 190:818
11. Gumpu MB, Nesakumar N, Sethuraman S, Krishnan UM, Rayappan JBB (2014) Sens Actuators B Chem 199:330
12. Küçük A, Torul O (2018) Synth Met 237:23
13. Lee MY, Wu CC, Sari MI, Hsieh YH (2018) Electrochim Acta 283:772
14. Kaçar C, Erden PE, Dalkıran B, İnal EK, Kılıç E (2020) Anal Bioanal Chem 412:1933
15. Dalkıran B, Erden PE, Kaçar C, Kılıç E (2019) Electroanal 31:1324
16. Erden PE, Erdoğan ZÖ, Öztürk F, Koçoğlu İO, Kılıç E (2019) Electroanal 31:2368
17. Pérez-López B, Merkoçi A (2011) Trends Food Sci Tech 22:625
18. Zeng Y, Zhu Z, Du D, Lin Y (2016) J Electroanal Chem 781:147
19. Pérez S, Bartrolí J, Fàbregas E (2013) Food Chem 141:4066
20. Hernández-Cázares AS, Aristoy MC, Toldrá F (2011) J Food Eng 106:166
21. Apetrei I, Apetrei C (2016) Sensors 16:422
22. Mehmeti E, Stanković DM, Chaiyo S, Švorc Ľ, Ortner A, Kalcher K (2016) Monatsh Chem 147:1161
23. Turkmen E, Bas SZ, Gulce H, Yildiz S (2014) Electrochim Acta 123:93
24. Jiang X, Wu Y, Mao X, Cui X, Zhu L (2011) Sens Actuators B Chem 153:158
25. Li J, Yu J, Wei X, Liu R (2011) J Solid State Electr 15:1129
26. Barquero-Quirós M, Domínguez-Renedo O, Alonso-Lomillo MA, Arcos-Martínez MJ (2012) Microchim Acta 179:65
27. Xu S, Qin X, Zhang X, Zhang C (2015) Microchim Acta 182:1241
28. Zou Y, Xiang C, Sun LX, Xu F (2008) Biosens Bioelectron 23:1010
29. Eremia SA, Vasilescu I, Radoi A, Litescu SC, Radu GL (2013) Talanta 110:164
30. Wang J (2006) Analytical electrochemistry, 3rd edn. John Wiley & Sons Inc, Hoboken
31. Agrisuelas J, González-Sánchez MI, Valero E (2017) Sens Actuators B Chem 249:499
32. Lange J, Wittmann C (2002) Anal Bioanal Chem 372:276
33. Eguilaz M, Agüí L, Yanez-Sedeno P, Pingarron JM (2010) J Electroanal Chem 644:30
34. Serra B, Morales MD, Reviejo AJ, Hall EH, Pingarron JM (2005) Anal Biochem 336:289
35. Compagnone D, Isoldi G, Moscone D, Palleschi G (2001) Anal Lett 34:841
36. Telsnig D, Kalcher K, Leitner A, Ortner A (2013) Electroanal 25:47
37. Leonardo S, Campàs M (2016) Microchim Acta 183:1881
38. Fang B, Wei Y, Li M, Wang G, Zhang W (2007) Talanta 72:1302